Thin Solid Films 774 (2023) 139819

Contents lists available at ScienceDirect

Thin Solid Films

journal homepage: www.elsevier.com/locate/tsf

High-sensitivity IR to UV broadband ellipsometry and transmission characterization of high-purity glasses

Andreas Furchner [a,*], Jörg Rappich [b], Sonya Calnan [c], Karsten Hinrichs [d], Sven Peters [e]

[a] Helmholtz-Zentrum Berlin für Materialien und Energie GmbH, Division Energy and Information, Schwarzschildstraße 8, 12489 Berlin, Germany
[b] Helmholtz-Zentrum Berlin für Materialien und Energie GmbH, Institut für Silizium-Photovoltaik, Kekuléstraße 5, 12489 Berlin, Germany
[c] Helmholtz-Zentrum Berlin für Materialien und Energie GmbH, PVcomB, Schwarzschildstraße 3, 12489 Berlin, Germany
[d] Leibniz-Institut für Analytische Wissenschaften – ISAS – e. V., Schwarzschildstraße 8, 12489 Berlin, Germany
[e] SENTECH Instruments GmbH, Schwarzschildstraße 2, 12489 Berlin, Germany

ARTICLE INFO

Keywords:
Broadband ellipsometry
Transmission absorption spectroscopy
Backside reflections
Spectral optical constants
Fused silica
Fused quartz
Suprasil 1
Herasil 102
Optical glasses
Dielectric function
Infrared spectroscopy

ABSTRACT

Glasses are widely used as transparent substrates in thin-film and optical applications, but also as window materials in devices and *operando* cells. Determining the dielectric properties of the glass over a wide spectral range is often the crucial first step for the subsequent quantitative spectroscopic analysis, design and application of layer stacks and complex sample systems. Reflection-based ellipsometry—the method of choice for this task—is challenging for thick transparent substrates because of backside reflections that influence the optical response. Here, we extend the methodological treatment of backside reflections in ellipsometry by accounting for the spatial overlap—and its dependence on incidence angle, thickness and refractive index—between the light beams' cross-sections and the detector aperture. We thereby demonstrate the incorporation of backside reflections in high-sensitivity multi-instrument, multi-angle ellipsometry and transmission for both measurement and quantitative modeling of glasses. Consolidating data from three instruments, we determine the dielectric function of two high-purity fused silica (Suprasil 1) and quartz (Herasil 102) glasses from the deep-ultraviolet to the mid-infrared (200–25000 nm), with a sensitivity to absorption features as small as 10^{-7}. Our non-destructive approach obviates the need for sample modifications like backside roughening, thus laying the foundation for future detailed ellipsometry studies on lower-purity glasses such as soda–lime- and borosilicate-based substrates for thin-film applications.

1. Introduction

Broadband ellipsometry has attracted interest from various fields of research and industry as a powerful optical technique for quantifying thicknesses and Kramers–Kronig consistent optical functions of thin films or bulk systems. Using polarized light, the method measures the change in polarization state of light upon interaction with a sample, expressed by the ellipsometric angles Ψ and Δ [1–3].

Glasses are ubiquitous materials for substrates and windows in thin-film systems, optical devices and flow cells [4,5]. Their optical properties are deceptively simple but often crucial to be determined accurately over a broad spectral range [6]. Such characterization usually constitutes the first step in the modeling process of complex layer stacks or *in situ* experiments such as film deposition or reactions at solid–liquid interfaces.

Glasses are transparent over a wide spectral range, which poses a challenge for spectroscopic measurements in reflection geometries. Depending on the glass thickness, light reflected from the sample backside can reach the detector and complicate the quantitative interpretation of the ellipsometric data. What is more, the spatial overlap between frontside and backside reflections depends on both the sample thickness, the incidence angle, the instrument's opening angle and aperture settings, as well as the optical properties of the glass.

Besides blocking unwanted reflections [7] (which can work for thick enough glasses), wedge samples or sample modifications such as backside roughening or the application of index-matching tapes or liquids are therefore routinely used to suppress backside reflections [1,8,9]. However, the measurement and characterization of glass-based samples and devices often has to be performed over a broad spectral range and in a non-destructive fashion. In fact, the latter is a strong point for which ellipsometry is widely known, praised and advertised. Moreover, including backside reflections in measurements and optical modeling can help to better account for influences of the instrument optics on the data.

* Corresponding author.
E-mail address: andreas.furchner@helmholtz-berlin.de (A. Furchner).

https://doi.org/10.1016/j.tsf.2023.139819
Received 30 September 2022; Received in revised form 9 March 2023; Accepted 28 March 2023
Available online 31 March 2023

Backside reflections in ellipsometry can be treated mathematically by approximating light source, light beams and detector to be point-like, having no spatial spread and no opening angle [10]. These assumptions work well for certain measurement geometries such as fixed incidence angles. In this article, we expand this approach and aim to determine the optical properties of glasses—the refractive and absorptive indices n and k related to the dielectric function $\varepsilon = (n + ik)^2$—whilst taking into account non-point-like backside reflections, their displacement in dependence of incidence-angle, thickness and refractive index, the consequent changing overlap with the detector aperture, and the treatment of non-zero opening angles in multi-incidence-angle ellipsometric data measurement and modeling.

Our study focuses on high-purity fused silica (Suprasil 1) and fused quartz (Herasil 102). The refractive and absorptive properties of such types of glasses have been investigated over a wide spectral range with various techniques including reflection, transmission, ellipsometry, interferometric, minimum-deviation, and Kramers–Kronig based analysis methods [6,11]. However, the reported optical constants vary quite substantially. These variations cannot be fully attributed to differences in the glass properties between different samples, but rather likewise indicate method-related or -intrinsic uncertainties and inaccuracies. Broadband multi-angle ellipsometry under consideration of non-point-like backside reflections could therefore prove to be a comprehensive method for reaching an improved level of data quality and accuracy.

We perform broadband multi-angle ellipsometry of Suprasil 1 and Herasil 102 glasses on multiple instruments and spectral ranges from the mid-infrared (mid-IR) to the deep-ultraviolet (deep-UV) [400–50 000 cm^{-1}; 25.0–0.2 µm], highlighting the impact of backside reflections on Ψ and Δ spectra in transparent spectral regions. Combining amplitude and phase with complementary transmission measurements pinpoints even small absorption features as low as 10^{-7} in k.

This work lays the foundation for future studies on thin films deposited on glasses with more complicated optical properties, such as soda–lime and borosilicate float glasses. These types of glasses are characterized by metal diffusion into the float side of the sample, rendering the properties of the two glass surfaces and sub-surface layers optically different. Including both frontside and backside reflections in the optical response is expected to increase the sensitivity of the ellipsometric measurements towards the diffusion profile and thus improve the accuracy of the optical model.

2. Experimental

2.1. Materials

Fused silica glass (Suprasil 1®, 220 µm thick) and fused quartz glass (Herasil 102®, 6015 µm thick) were obtained from Heraeus. The thicknesses were determined with a micrometer gauge to ±3 µm.

2.2. Ellipsometry and transmission set-ups

Comprehensive measurements at room temperature were conducted in the SENTECH Thin Film Metrology Application Lab and in the Application Lab for Infrared Ellipsometry at ISAS. First, broadband IR transmission measurements (400–8000 cm^{-1}; 25.00–1.25 µm) were performed in the sample compartment of an FTIR spectrometer (Bruker Tensor 37). Second, an FTIR-based ellipsometer (SENDIRA, SENTECH Instruments) was employed for ellipsometry in the mid-IR range (400–6666 cm^{-1}; 25.0–1.5 µm). Third, broadband ellipsometry and transmission measurements were performed on a NIR–Vis–UV ellipsometer (SENresearch 4.0, SENTECH Instruments) that covers a wide spectral range from the near-IR (2.50 µm) up to the deep-UV (0.19 µm).

The glasses were measured in transmission at normal incidence. Ellipsometric Ψ and Δ spectra were acquired at multiple incidence angles. Neither special sample nor optics modifications were applied with respect to backside reflections.

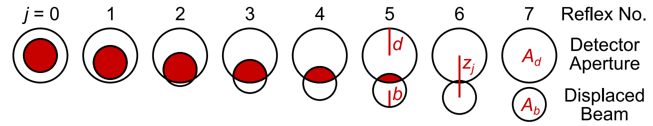

Fig. 1. Schematic illustration of the jth displaced (by z_j) backside reflection (area A_b) and its (partial) overlap with the detector aperture (area A_d). $j = 0$ refers to the frontside reflex.

2.3. Optical modeling

The broadband ellipsometry and transmission data were evaluated in SpectraRay/4 (SENTECH Instruments) using an optical model of a thick incoherent glass slab with surface roughness layers (equal thicknesses) on either side, described by a Bruggeman effective medium approximation of 50% glass and 50% air.

Ellipsometry and transmission data from the different instruments and spectral ranges (MIR, NIR, Vis–UV) were quantified with a broadband optical layer model. However, the differences of the optical set-ups (opening angles, beam diameters, apertures, etc.) were treated individually in order to accurately model the impact of the different instrument functions on the data.

Backside reflections were accounted for in the incoherent calculation [3] by including a sufficient number of multiple reflections within the thick glass layer. These reflections are displaced with respect to the frontside reflection beam according to the incidence angle φ as well as the thickness h and the complex refractive index $N = n + ik$ of the glass. The result is a φ-, h- and N-dependent overlap between the reflected beams and the detector aperture, described by corresponding diameters in the simulation.

In detail, for a plane-parallel sample of thickness h and complex refractive index N_ϑ, the beam displacement z_j (perpendicular to the beam propagation) for the jth backside reflection in dependence of the incidence angle φ is given by

$$z_j(\varphi, h, N_\varphi, N_\vartheta) = 2h \cdot j \cdot \cos\varphi \tan\vartheta, \tag{1}$$

where ϑ (the transmission angle within the thick layer) is calculated from Snell's law according to

$$N_\vartheta \sin\vartheta = N_\varphi \sin\varphi. \tag{2}$$

N_φ is the ambient's complex refractive index ($N_\varphi = 1$ for air). As illustrated in Fig. 1, the fraction $F(z_j)$ of light that can reach the detector ($0 \le F \le 1$) depends on the overlap of the circular cross-section A_b of the displaced beam of radius b with the area A_d of the detector aperture of radius d. For $|b - d| < z < b + d$, the overlap of A_b and A_d (highlighted area in Fig. 1) normalized to the illuminated detector area without beam displacement is found to be given by:

$$F(z_j) = \frac{S}{\min(A_b, A_d)} \left[b^2 \operatorname{acos}\frac{z_j^2 + b^2 - d^2}{2 z_j b} + d^2 \operatorname{acos}\frac{z_j^2 + d^2 - b^2}{2 z_j d} - \frac{1}{2}\sqrt{(b + d - z_j)(z_j + b - d)(z_j - b + d)(z_j + b + d)} \right]$$

Here, S is an additional damping factor ($0 \le S \le 1$) that can be introduced to describe scattering losses and related effects upon reflection at the sample backside. Each backside beam j is weighted by $F(z_j)$ in the incoherent summation.

The above approach can be readily extended to account for non-uniform sample/detector illumination, such as from Gaussian beam profiles of laser sources, from elliptical or other beam shapes, or from wedge-shaped samples. Also the special case of narrow samples can be treated by accounting for the finite sample width that might prevent the jth reflected backside beam to leave the sample and reach the detector.

Circular apertures equivalent to the radii $b = 1.5$ mm and $d = 2.4$ mm were employed in the input arm and on the detector side of the Vis–UV ellipsometer. The beam of the NIR–Vis–UV ellipsometer was treated

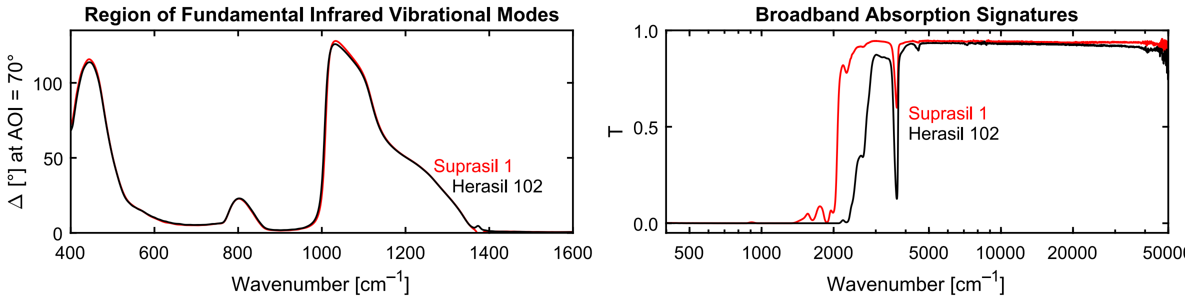

Fig. 2. Measured mid-IR ellipsometric phase (Δ) spectra at an angle of incidence (AOI) of 70° (left) and broadband (MIR–NIR–Vis/UV) transmission (T) spectra (right) of the two glass samples, showing the ranges of strong and weak absorption, respectively.

as non-divergent in the model. The used IR ellipsometer, on the other hand, focuses a larger beam, equivalent to $b = 4$ mm on the input side, with an opening angle of about $\varphi_{OA} = 5.6°$. This angle was accounted for in the model by averaging intensities calculated at multiple angles around $\varphi \pm \varphi_{OA}$ in Stokes parameter space before the conversion into the ellipsometric parameters Ψ and Δ. For the investigated glass samples, the first three backside reflections were included in the model. Higher-order reflections are strongly suppressed because of Fresnel reflection losses and/or damping due to absorption within the glass.

3. Results and discussion

The purities of fused silica and fused quartz are extremely high. Both types of glass consist of pure SiO_2 with small amounts of impurities in the form of metal oxides (such as Al_2O_3, Fe_2O_3, TiO_2, MgO, and ZrO), Na, chlorine, and water (present as OH groups). Fused silica glasses have a lower number of metallic contaminants and are consequently slightly more pure than fused quartz glasses. Depending on the preparation process, the amount of OH in fused silica is typically lower than 1300 ppm [12]. Fused quartz exhibits a very high glass transition temperature of about 1200 °C and usually an even lower OH content <250 ppm [13]. The small differences in composition impact the optical properties of the glasses, particularly in the mid-IR spectral range.

3.1. Refractive and absorptive properties

Understanding the refractive and absorptive properties of the glasses is a prerequisite for building a physically meaningful optical model. We begin our analysis by introducing the characteristic absorption features in the mid-IR/near-IR region and then turn to the quantitative evaluation of the multi-angle broadband spectroscopic data, including backside reflections.

Fig. 2 shows measured Δ spectra at 70° incidence angle in the low mid-IR range, as well as broadband transmission spectra up to the deep-UV. Within the considered MIR–UV spectral range, fused silica and fused quartz glasses have a wide transparent window in the NIR–Vis–UV where absorption is negligibly small. The optical response in this window is dominated by the glasses' dispersive properties. The absorptive properties become relevant mainly in the infrared range where the two glasses exhibit characteristic vibrational fingerprints.

Dominant bands of amorphous SiO_2 in the 400–1600 cm^{-1} range are related to the fundamental strong IR vibrational modes of the glass matrix—for instance, bending modes around 450 cm^{-1}, symmetric stretching modes around 810 cm^{-1}, asymmetric in-phase stretching modes at about 1080 cm^{-1}, and asymmetric out-of-phase stretching modes at about 1190 cm^{-1} (assignments according to Refs. [11,14]).

The 1300–8000 cm^{-1} range covers a vast array of combination and overtone modes of SiO_2 as well as modes due to impurities, hydroxyl (OH) inclusions and concomitant hydrogen-bonding effects. A comprehensive band discussion for fused silica can be found in Ref. [11], which assigns a series of combination modes and overtones of the silica matrix.

A prominent characteristic OH-related feature in Fig. 2 is the relatively sharp band at about 3680 cm^{-1} [15,16], found for both Suprasil 1 and Herasil 102. Considering the thicknesses of the two glasses (220 μm and 6015 μm, respectively), the amplitudes of this band reflect the expected OH content in these synthetic glasses.

3.2. Broadband multi-instrument analysis

For bulk samples that can be optically described as a semi-infinite substrate, it is in principle sufficient to perform ellipsometry at a single incidence angle when aiming at the extraction of n and k data. For transparent substrates, however, there are two main challenges in the modeling process, namely the correct treatment of backside reflections and the joining of the separate spectral ranges from different instruments.

Relatively thin samples such as the 220 μm thick Suprasil 1 glass displace the backside reflection beams only slightly. For the much thicker (6 mm) Herasil 102 glass, there is a substantial and non-negligible beam displacement on the order of millimeters, leading to a reduced overlap between beam and detector aperture. In the infrared, this overlap is complicated by the focusing optics, that is, by the instrument's opening angle of about 5.6°. Multi-angle measurements, especially around the Brewster angle, are therefore indispensable for decorrelating the effects of the different ellipsometer instrument functions on the ellipsometric data.

Measured and fitted broadband multi-angle ellipsometry and transmission spectra of the Herasil 102 sample are shown in Fig. 3. The influence of backside reflections becomes visible in regions of low absorption (high transmission), for instance, in the form of elevated baselines in Ψ [9]. For Δ, there are spectral shifts of the Brewster-angle-related phase jumps between 0° and 180°. The baseline effects are not discernible on the level of the measured spectra in the NIR–Vis–UV region due to the lack of spectral contrast in the absence of absorption features in this range. However, baseline alterations in Ψ are clearly apparent in the mid-IR data, for example, below and above the semi-transparent spectral region around 3680 cm^{-1}.

In modeling the optical response of the glasses, their dielectric functions receive different contributions from various absorption and refraction properties. Although absorption is insignificant for the Suprasil 1 sample towards the deep-UV end of the considered spectral range, there is a measurable dispersion originating from absorption at even higher energies. A Tauc–Lorentz dispersion with a band gap around 8.5 eV [17] was used to describe this UV absorption edge of the amorphous glasses and the resulting dispersion tail at lower energies. For the Herasil 102 sample, the very small absorption features below 250 nm, related to impurities within the glass, were modeled using Gaussian oscillators. The samples' rich vibrational mid-IR/near-IR fingerprints were modeled using a sum of Voigt oscillators—a convolution of Lorentzian with Gaussian bandshapes. Their Gaussian band broadening represents the frequency distribution of oscillators associated with disorder in the amorphous glass structures [11]. Of predominantly

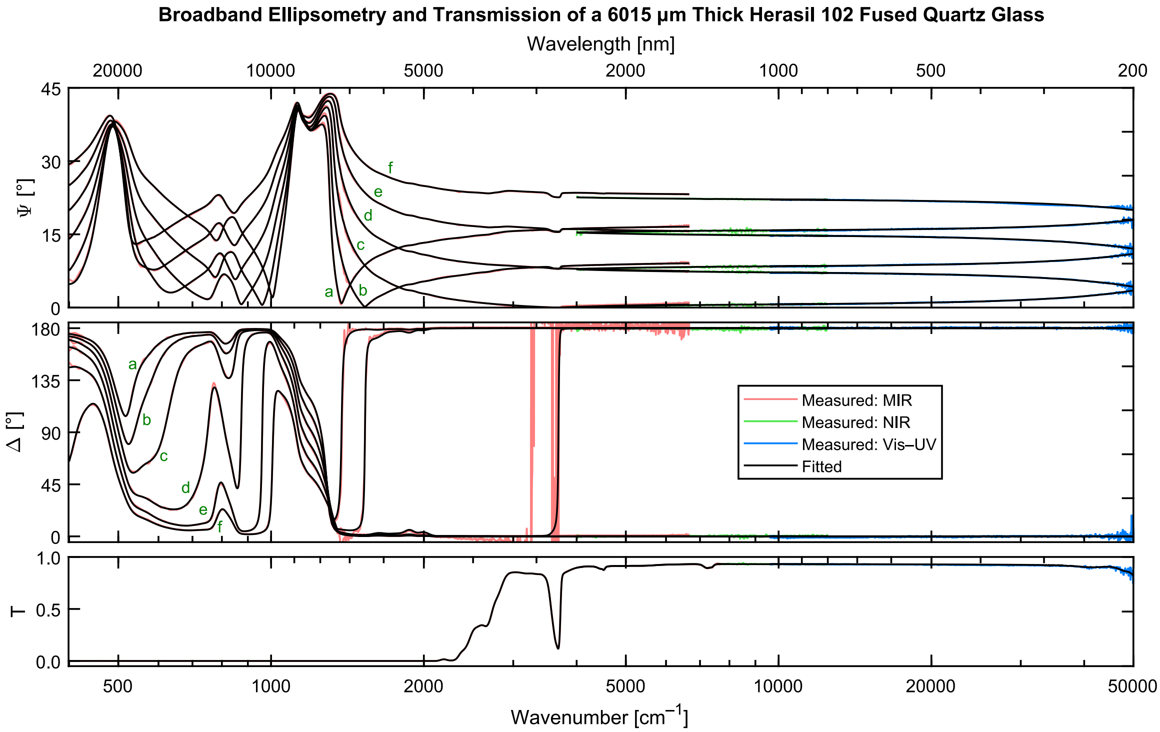

Fig. 3. Measured and fitted broadband (MIR–NIR–Vis/UV) ellipsometry (Ψ, Δ) and transmission (T) spectra of the 6 mm thick Herasil 102 fused quartz glass sample at incidence angles between 45° (a) and 70° (f) in 5° steps.

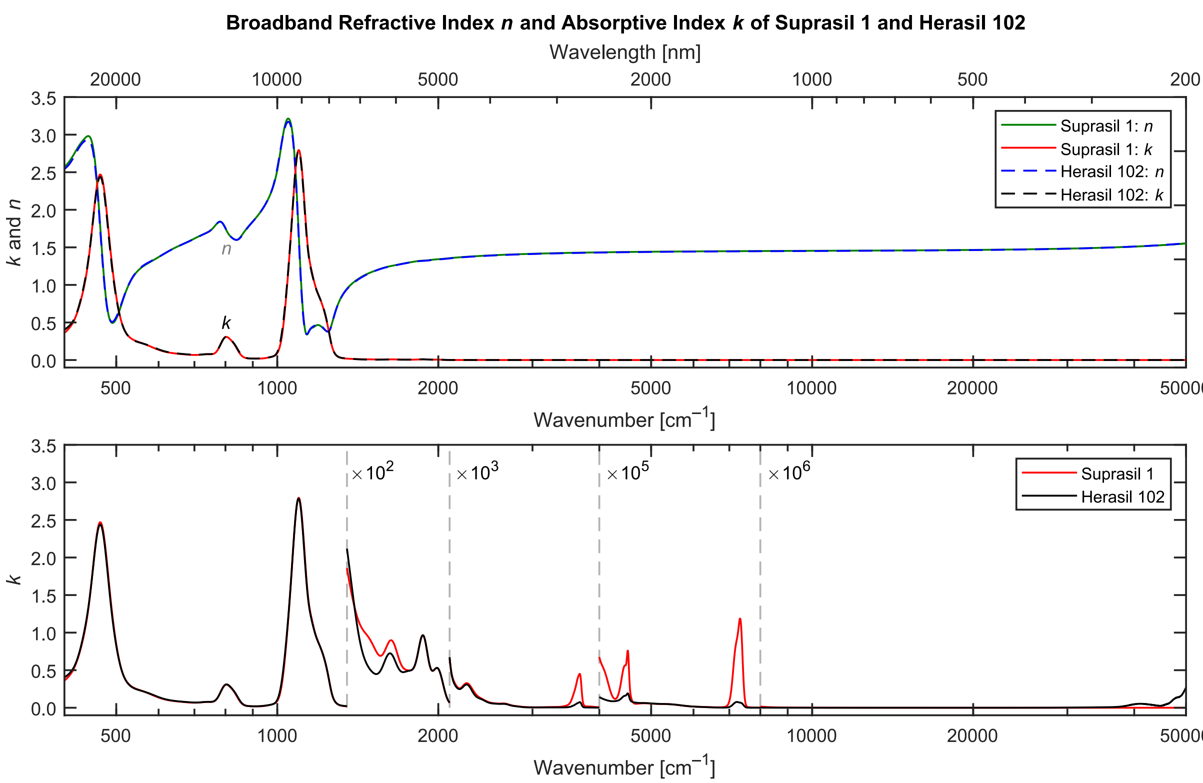

Fig. 4. Broadband refractive index n and absorptive index k of Suprasil 1 fused silica and Herasil 102 fused quartz glass.

Gaussian profile are the IR absorption bands that arise from the fundamental and combination/overtone vibrational modes of the glass matrix.

Importantly, every vibrational band—and thus its associated oscillator in the model—has a dispersion tail and leads to a contribution to the refractive index at higher energies. Therefore, even the small vibrational features in the mid-IR/near-IR range must be accounted for in order to obtain correct ellipsometric baselines. These small bands can be measured more accurately in transmission. It is hence the combination of ellipsometry and transmission measurements that facilitates the modeling of the transition from the mid-IR with its strong absorption bands, to the NIR with its rather weak combination, overtone and inclusion bands, to the non-absorbing Vis–UV range.

Except for a phase jump around $3635\,cm^{-1}$ in Δ at 55° (curve c), Fig. 3 shows that the optical model reproduces the measured multi-angle data. This demonstrates that effects from the interplay of backside reflections and instrument function on ellipsometric spectra can be described by the presented approach. The observed phase behavior indicates that the glass front- and backside exhibit surface regions with a slightly higher refractive index than the bulk (on the order of $\delta n \approx 0.0001$ or less). Among other potential reasons, this could be a result of the polishing process. Surface roughnesses, as obtained from the fit, are less than 0.1 nm on both sides of the glass, which is in accordance with the sample specifications.

The optical constants of the two glasses that result from the broadband fit are presented in Fig. 4. In combination with transmission measurements, the ellipsometric analysis is able to reveal even small absorption features as tiny as 10^{-7} or lower in k.

The dielectric properties of the fundamental vibrations in the mid-IR below $1300\,cm^{-1}$ are quite similar for both glass samples. However, there are substantial relative differences in k above $1300\,cm^{-1}$ related to the glass compositions. Suprasil 1 is a fused silica material manufactured by flame hydrolysis of $SiCl_4$, whereas Herasil 102 is fabricated by flame fusion of cultured quartz crystals. While Suprasil 1 contains fewer impurities than Herasil 102, it does contain more OH groups, as previously discussed. Take, for example, the OH-associated bands around $3680\,cm^{-1}$ and $4500\,cm^{-1}$. Their corresponding oscillator amplitudes correlate with the amount of hydroxyl groups within the glasses [15]. The fit reveals a difference in OH content by a factor of 5.8, which again is consistent with the sample specs (<1300 ppm for Suprasil 1 [12], ≈150 ppm for Herasil 102 [13]).

4. Conclusions and outlook

We performed a broadband multi-angle ellipsometry and transmission study of the optical properties of thick glass samples that incorporates backside reflections occurring in transparent spectral regions. It was shown that spectral multi-angle data from multiple ellipsometers and spectrometers can be consolidated and interpreted quantitatively when properly accounting for the displaced backside reflections in combination with the instruments' opening angle and aperture settings. Complementary transmission and ellipsometric measurements enabled the accurate analysis of spectral ranges with low absorption as small as 10^{-7} in k.

This work has implications for future investigations and modeling of thin-film systems with optically complicated glasses such as float glasses that exhibit different frontside and backside optical properties. The ellipsometric methodology is also promising for the analysis of new materials like metallic glasses [18,19], which are increasingly used in the fields of nanotechnology, medical technology and catalysis.

CRediT authorship contribution statement

Andreas Furchner: Conceptualization, Methodology of broadband measurements, Data acquisition, Data evaluation, Writing – original draft & editing, Visualization. **Jörg Rappich:** Sample preparation, Writing – review. **Sonya Calnan:** Rescources, Writing – review. **Karsten Hinrichs:** Data interpretation, Rescources, Writing – review. **Sven Peters:** Methodology of Measurements, Data Interpretation, Data Evaluation, Rescources, Writing – review.

Declaration of competing interest

The authors declare that they have no known competing financial interests or personal relationships that could have appeared to influence the work reported in this paper.

Data availability

Data underlying the results presented in this paper are not publicly available at this time but may be obtained from the authors upon reasonable request.

Acknowledgments and funding

We thank Mike Hoffmann and Timur Shay for software support and the fast implementation of Voigt oscillators in the SpectraRay/4 measurement and analysis software. We particularly thank Uwe Richter for valuable discussions and support regarding the treatment of backside reflections. Funding is gratefully acknowledged: Application Lab for Infrared Ellipsometry via the Europäischer Fonds für regionale Entwicklung (EFRE, 1.8/13); Ministerium für Kultur und Wissenschaft des Landes Nordrhein-Westfalen; Die Regierende Bürgermeisterin von Berlin – Senatsverwaltung Wissenschaft, Gesundheit, Pflege und Gleichstellung; Bundesministerium für Bildung und Forschung. The authors acknowledge support from the Federal Ministry of Education and Research in the framework of the project CatLab, Germany (03EW0015A/B).

References

[1] H.G. Tompkins, E.A. Irene, Handbook of Ellipsometry, William Andrew, Inc., Norwich, 2005, URL http://www.sciencedirect.com/science/book/9780815514992.
[2] K. Hinrichs, K.-J. Eichhorn, Ellipsometry of Functional Organic Surfaces and Films, Springer-Verlag Berlin Heidelberg, 2018, http://dx.doi.org/10.1007/978-3-319-75895-4.
[3] H. Fujiwara, Spectroscopic Ellipsometry: Principles and Applications, John Wiley & Sons, Ltd, Chichester, ISBN: 978-0-470-01608-4, 2007, http://dx.doi.org/10.1002/9780470060193.
[4] K. Saito, A.J. Ikushima, Glasses as engineering materials: A review, Mater. Des. 32 (4) (2011) 1717–1732, http://dx.doi.org/10.1016/j.matdes.2010.11.057.
[5] L.A. Moore, C.M. Smith, Fused silica as an optical material, Opt. Mater. Express 12 (8) (2022) 3043–3059, http://dx.doi.org/10.1364/OME.463349.
[6] R. Kitamura, L. Pilon, M. Jonasz, Optical constants of silica glass from extreme ultraviolet to far infrared at near room temperature, Appl. Opt. 46 (33) (2007) 8118–8133, http://dx.doi.org/10.1364/AO.46.008118.
[7] R.A. Synowicki, B.D. Johs, A.C. Martin, Optical properties of soda-lime float glass from spectroscopic ellipsometry, Thin Solid Films 519 (2011) 2907–2913, http://dx.doi.org/10.1016/j.tsf.2010.12.110.
[8] D.J. Hayton, T.E. Jenkins, On the frustration of back-surface reflection from transparent substrates in ellipsometry, Meas. Sci. Technol. 15 (2) (2003) N17–N20, http://dx.doi.org/10.1088/0957-0233/15/2/N01.
[9] R.A. Synowicki, Suppression of backside reflections from transparent substrates, Phys. Status Solidi C 5 (5) (2008) 1085–1088, http://dx.doi.org/10.1002/pssc.200777873.
[10] B. Johs, R. French, F. Kalk, W. McGahan, J. Woollam, Optical analysis of complex multilayer structures using multiple data types, in: Proceedings of SPIE 2253, Optical Interference Coatings, 1994, pp. 1098–1106, http://dx.doi.org/10.1117/12.192054.
[11] A.M. Efimov, V.G. Pogareva, IR absorption spectra of vitreous silica and silicate glasses: The nature of bands in the 1300 to 5000 cm^{-1} region, Chem. Geol. 229 (1–3) (2006) 198–217, http://dx.doi.org/10.1016/j.chemgeo.2006.01.022.
[12] Heraeus, Quartz glass for optics – data and properties, 2022, https://www.heraeus.com.
[13] Wisag, Quarzglas für die optik – daten und eigenschaften, 2022, https://www.wisag.ch.
[14] C.T. Kirk, Quantitative analysis of the effect of disorder-induced mode coupling on infrared absorption in silica, Phys. Rev. B 38 (2) (1988) 1255–1273, http://dx.doi.org/10.1103/PhysRevB.38.1255.
[15] C.L. Losq, G.D. Cody, B.O. Mysen, Complex IR spectra of OH^- groups in silicate glasses: implications for the use of the 4500 cm^{-1} IR peak as a marker of OH^- groups concentration, Am. Mineral. 100 (4) (2015) 945–950, http://dx.doi.org/10.2138/am-2015-5076.
[16] A.K. Islamov, E.M. Ibragimova, B.S. Faizullaev, E.T. Ruziev, Infrared spectra of KU1 and KS-4V quartz glass irradiated by fast neutrons, Glass Phys. Chem. 44 (6) (2018) 551–556, http://dx.doi.org/10.1134/S1087659618060093.
[17] K. Saito, A.J. Ikushima, Absorption edge in silica glass, Phys. Rev. B 62 (13) (2000) 8584–8587, http://dx.doi.org/10.1103/PhysRevB.62.8584.
[18] Z. Jia, X. Duan, W. Zhang, W. Wang, H. Sun, S. Wang, L.-C. Zhang, Ultra-sustainable $Fe_{78}Si_9B_{13}$ metallic glass as a catalyst for activation of persulfate on methylene blue degradation under UV-vis light, Sci. Rep. 6 (38520) (2016) http://dx.doi.org/10.1038/srep38520.
[19] V. Hasannaeimi, S. Mukherjee, Noble-metal based metallic glasses as highly catalytic materials for hydrogen oxidation reaction in fuel cells, Sci. Rep. 9 (12136) (2019) http://dx.doi.org/10.1038/s41598-019-48582-7.